Int. J. Heat Mass Transfer. Vol. 14, pp. 365–375. Pergamon Press 1971. Printed in Great Britain

TURBULENT FLOW IN NON-CIRCULAR DUCTS. PART 1

MEAN FLOW PROPERTIES IN THE DEVELOPING REGION OF A SQUARE DUCT

S. AHMED* and E. BRUNDRETT

Department of Mechanical Engineering, University of Waterloo, Waterloo, Ontario, Canada

(*Received* 21 *November* 1969 *and in revised form* 7 *May* 1970)

Abstract—The generalized mean properties of turbulent flow in non-circular ducts are examined for the developing region of a square duct. The experimental data include mean velocity profiles and peripheral wall shear distributions at several locations, as well as the longitudinal static pressure distribution, all for Reynolds numbers between 50 000 and 150 000.

A similarity exists between the mean wall isovels and peripheral wall shear distributions in the developing region with those of fully developed flow. The wall shear stress rapidly assumes a value that is slightly greater than that for fully developed flow, even though the axial pressure gradient has not stabilized, due to the convective acceleration of the core fluid. This indicates that the near wall flow rapidly establishes fully developed properties.

It is recommended that for engineering calculations an effective development length in conduits be defined in terms of the stabilization of wall parameters such as shear stress and heat transfer. For this square duct with a well-rounded large contraction ratio entrance, the wall shear stress had established within six hydraulic diameters, while by comparison the core fluid required a development length approximately an order of magnitude larger, and would appear to be controlled more by the Reynolds number. The Preston tube experimental shear stress data are confirmed by a momentum integral procedure which is generalized for all regular polygons. The experimental and predicted wall shear stress data are correlated to within 4 per cent of fully developed pipe data by using a new characteristic length scale which takes into account the shape of the duct.

NOMENCLATURE

D, side length of regular polygon;
D_H, hydraulic diameter of regular polygon;
D_L, new characteristic length of regular polygon;
δ, boundary layer thickness;
x_1, x_2, x_3, cartesian co-ordinates;
U_1, velocity in the longitudinal direction;
U_E, entrance velocity;
U_M, mean velocity in duct = U_E (assumed uniform);
U_G, velocity outside the boundary layer (assumed uniform);
U_*, wall shear velocity;
dP, static pressure difference between two faces of slice dx_1;
τ_w, wall shear stress;
θ, half the included angle between sides of regular polygon;
ρ, mass density of fluid;
ν, kinematic viscosity of fluid;
Re, Reynolds number;
Re_H, Reynolds number based on $D_H = U_M D_H/\nu$;
Re_L, Reynolds number based on $D_L = U_M D_L/\nu$;
C_f, friction factor = $\tau_w/\frac{1}{2}\rho U_M^2$.

Velocity superscript '+' implies: velocity/$\sqrt{(\tau_w/\rho)}$.

Length superscript '+' implies: length $x\sqrt{(\tau_w/\rho)}/\nu$ where $\sqrt{(\tau_w/\rho)} = U_*$,

* Presently at SPAR Aerospace Products Ltd., Toronto, Ontario, Canada.

INTRODUCTION

THE EFFICIENT design of compact heat exchangers with non-circular passages demands that the turbulent flow characteristics be known in both the fully developed region as well as the developing region. In contrast to the extensive investigation of the flow over plates, and through circular pipes, a very small amount of data exists for flow in non-circular conduits. This is particularly true when we consider that each duct has certain unique properties, and that each duct could be investigated as completely as a circular pipe. It is however, the intention of the authors to relate the flow properties of non-circular ducts to those of pipes, with as general and yet as accurate correlation techniques as are possible. This is feasible since such parameters as wall shear stress and wall heat transfer are found to be dominated by the near wall flow, and are influenced to some extent by the duct shape.

For the case of a circular pipe the equations of motion adopt their simplest form, particularly for fully developed flow. A single velocity profile, which is sufficient to characterize the flow, can be obtained from a single auxiliary equation to express the turbulent shear stress distribution. The adoption of Prandtl's mixing length assumption as the auxiliary equation, along with the Couette flow assumption to simplify the equations of motion, yields the well known law of the wall or wall log law velocity profile. This profile, when it is assumed to apply for all of the pipe yields a drag law which is commonly used. Blasius [1] and others have proposed drag laws based upon power laws or other empirical correlations, with good results, but for a limited Reynolds number range.

Based on the success of drag laws for fully developed flow through circular pipes, attempts were made to extend the procedure to non-circular ducts. The pipe diameter was approximated by the hydraulic diameter and the observed friction factors calculated from the pipe law were found to be in error by as much as 30 per cent, depending on the shape of duct (Claiborne [2]). For square and triangular ducts, these errors were about 10 per cent. These results are not surprising considering the nature of turbulent flow in non-circular ducts.

Carlson and Irvine [3] working with a triangular duct at appropriate Reynolds numbers, varied the apex angle from 4° to 39° and showed that the error in the Blasius' friction formula varied from 20 to 4 per cent. These overall numerical observations were backed up by the experimental observations of Eckert and Irvine [4], which showed the existence of both laminar and turbulent regions in fully developed flow through a triangular duct. The extent to which the laminar region existed depended upon the Reynolds number.

Nikuradse [5] was possibly the first to establish the tendency of the isovels (equal velocity plots in the cross section) to penetrate the corner regions of non-circular ducts. Prandtl [6] explained the mechanism of this tendency of the flow on the basis that turbulent fluctuations were larger tangential to the isovel than normal. The resulting body force was greatest at the points of largest curvature of the isovels and acted in the direction of decreasing mean velocity. This thus gave a flow directed towards the corner, and by continuity required the flow to move along the straight boundaries and away at the point of smaller curvature resulting in a spiralling secondary motion. This pattern has been established experimentally by Hoagland [7] and Brundrett and Baines [8]. The latter reference cites square, rectangular, triangular and trapezoidal duct data and shows that the corner bisector separates the secondary flow cells. Deissler and Taylor [9] neglected the secondary flows and solved the non-circular duct problem by assuming the log law to hold along rays normal to the isovels. Their results for square and equilateral triangular ducts did not agree consistently with experimental results. The experimental data also did not correlate with circular pipe data, but was, in general, lower. The friction factors for the

square duct were lower by about 8 per cent and for the triangular duct by about 4 per cent. The heat transfer data showed the same trend and was lower in both cases by about 3 per cent for the square duct and about 8 per cent for the triangular duct.

It is thus seen that the circular pipe is a very special case of the general flow through arbitrary shaped ducts, even for the fully developed case. Hence in order to generalise the circular pipe drag and heat transfer laws, and to check turbulence models which are necessitated by new developments [10, 11] it is necessary to conduct investigations in a large number of non-circular ducts, both for the fully developed, as well as for the developing regions. In this paper the authors will consider the drag law requirements for the developing flow region of a square duct.

Experimental investigation of developing flow in a square duct

To obtain experimental data, a square duct tunnel was constructed as shown in Fig. 1. It consisted of a centrifugal blower, a settling chamber and the duct. The blower was capable of developing a total head of about $2\frac{1}{2}$ in. of water, and was connected through a rubber sleeve to the settling chamber. The rubber sleeve served to isolate any mechanical vibrations and also tended to even out any small pulsations in the flow. The diffusing section of the settling chamber had two screens to spread the flow. A tuft survey was carried out to ensure that no pulsating stall was present. The cylindrical portion of the settling chamber contained a hexagonal honey-comb followed by three damping screens. The contraction sections available were both gradual and sharp with a contraction ratio of 1:7·25. The end of the gradual contraction section had a $\frac{1}{16}$ in. wide peripheral sand paper strip to trip the flow at the entry to the duct. The duct was $3\frac{5}{8}$ in. square and was built of 2 ft lengths. The maximum ridge at the joints was less than 4 thousandth of an inch ensuring hydrodynamically smooth joints. The traversing mechanism was taken from a precision lathe and could locate the probes to within a thousandth of an inch.

The mean velocities were taken by traversing a Pitot-static tube connected to a Betz manometer. The Pitot-static tube had an outer diameter of 0·10 in. The isovels were found by surveying one octant of the $3\frac{5}{8}$ in. square duct at $\frac{1}{8}$ in. intervals. The data closest to the boundary were taken at a distance of $\frac{3}{16}$ in. from the wall. With reference to the work of MacMillan [12]

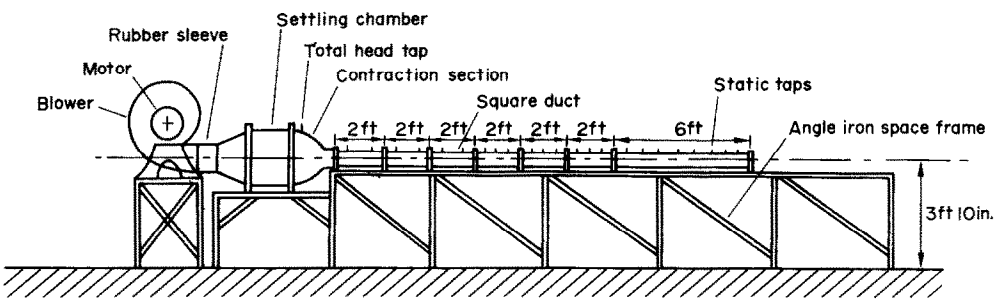

FIG. 1. Wind tunnel layout.

on Pitot tube effects on the readings, the distance from the wall was such that its effect was negligible. In the same paper it is mentioned that the effect of the shear region on the readings is equivalent to the Pitot tube being apparently displaced by 0·15 its diameter towards the higher velocity region. On the basis of this suggestion, the velocity readings presented in this paper have been over estimated in the highest shear region by a maximum of 0·75 per cent. The symmetry of the flow was checked by a survey of corresponding points in the other seven octants during the course of a run. Symmetry was present to within 3 per cent of the local flow. The mean flow field was found at four longitudinal locations and at four different Reynolds numbers at each location. The isovels presented in Fig. 2 are at four

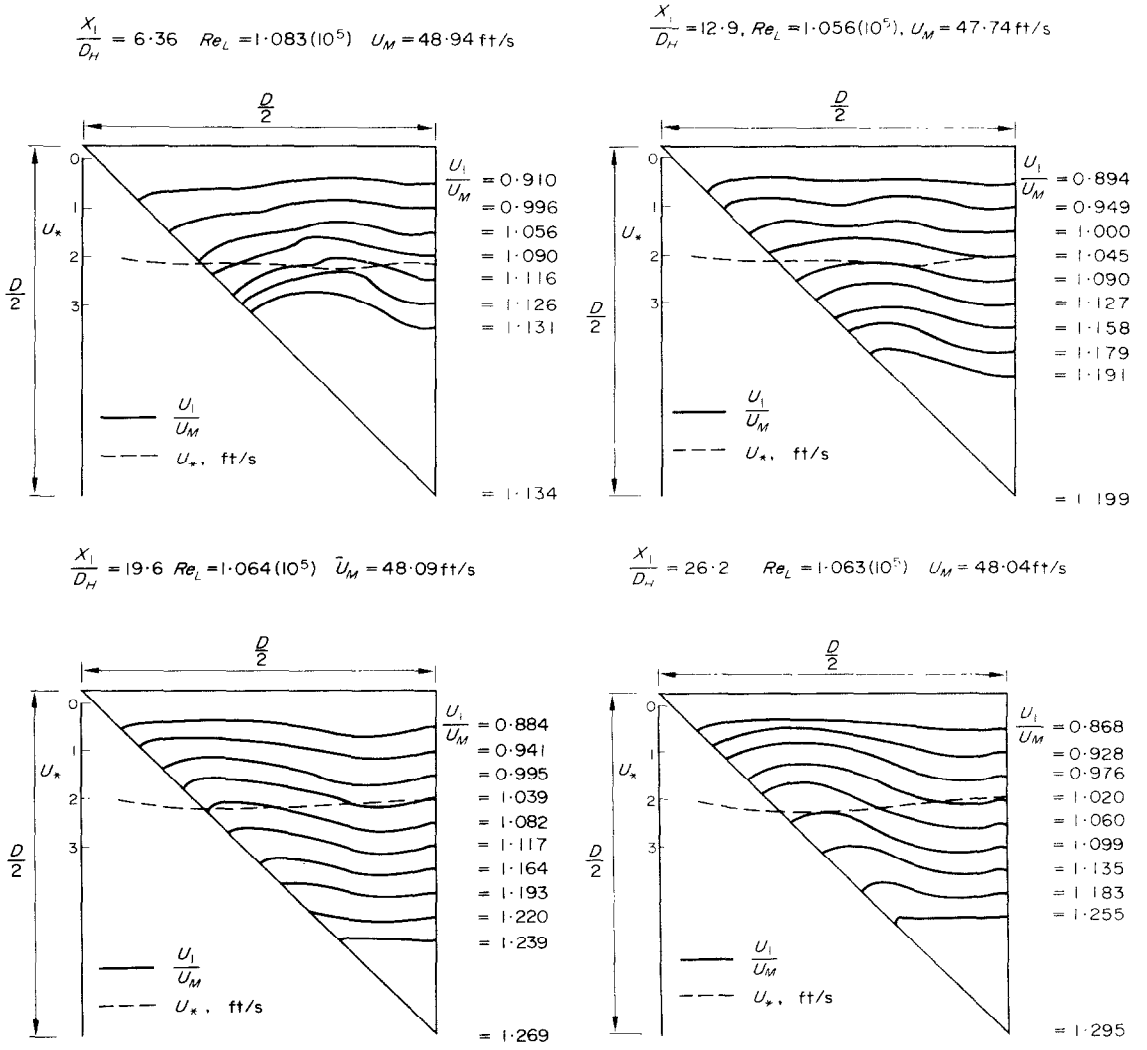

FIG. 2. Isovels and wall shear velocity (a) for $x_1/D_H = 6{\cdot}36$, $Re_L = 1{\cdot}083 \times 10^5$. (b) for $x_1/D_H = 12{\cdot}9$, $Re_L = 1{\cdot}056 \times 10^5$. (c) for $x_1/D_H = 19{\cdot}6$, $Re_L = 1{\cdot}064 \times 10^5$. (d) for $x_1/D_H = 26{\cdot}2$, $Re_L = 1{\cdot}063 \times 10^5$.

locations for a Reynolds number of about $1{\cdot}065 \times 10^5$ for a gradual entrance to the duct. The measuring apparatus was set up for each longitudinal location to obtain the readings for four Reynolds numbers. At subsequent locations, the intentions were to take readings at the same four Reynolds numbers. This was done by means of the total head reading in the settling chamber, using the entrance section as a calibrated flow nozzle. Thus the Reynolds number varies slightly from section to section, but is of no consequence to the isovel and shear stress data of Fig. 2.

It can be seen in Fig. 2 that the isovels curve away from the boundary as the diagonal is approached at an $x_1/D_H = 6{\cdot}36$, but become nearly parallel to the boundary at $x_1/D_H = 12{\cdot}9$. Further down-stream, at $x_1/D_H = 19{\cdot}6$ and at $26{\cdot}2$, there is an increasing tendency of the isovels to go nearer the boundary as the diagonal is approached. The isovel shape suggests that secondary flows exist in the developing region and that their influence consistently increases along the development length. Thus the structure of fully developed flow in a square duct manifests itself early in the development region, particularly with respect to corner penetration by the isovels.

The peripheral wall shear readings were taken with a Preston tube at each location and Reynolds number. The longitudinal pressure gradient (Fig. 3) was small enough that the use of the Preston tube was justified by Patel's correlation [13]. An important point to note

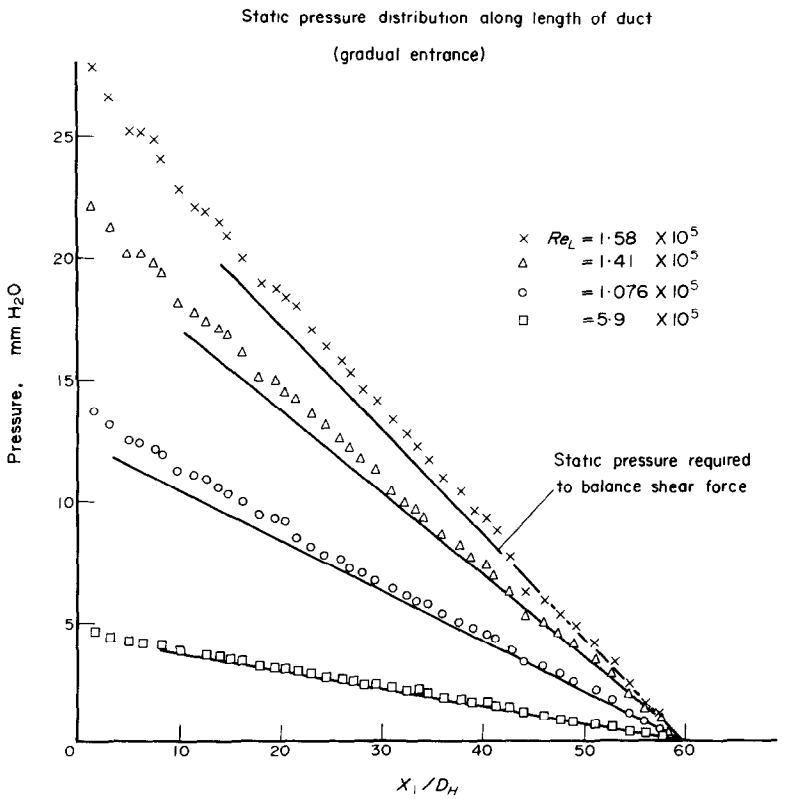

FIG. 3(a). Experimental static pressure distribution in the developing region for a gradual entrance.

from the isovels and wall shear velocity plots (Fig. 2) is that though the core flow is still developing with length, the average wall shear velocity has become nearly constant for a given Reynolds number. This illustrates that the value of the fully developed wall shear stress is obtained early in the developing length to increase as the Reynolds number increases. This can be detected since the pressure gradient is greater in the developing region than for fully developed flow, due to the acceleration of core fluid. The static pressure distribution is also presented for a sharp entry, in Fig. 3(b). The development length is still

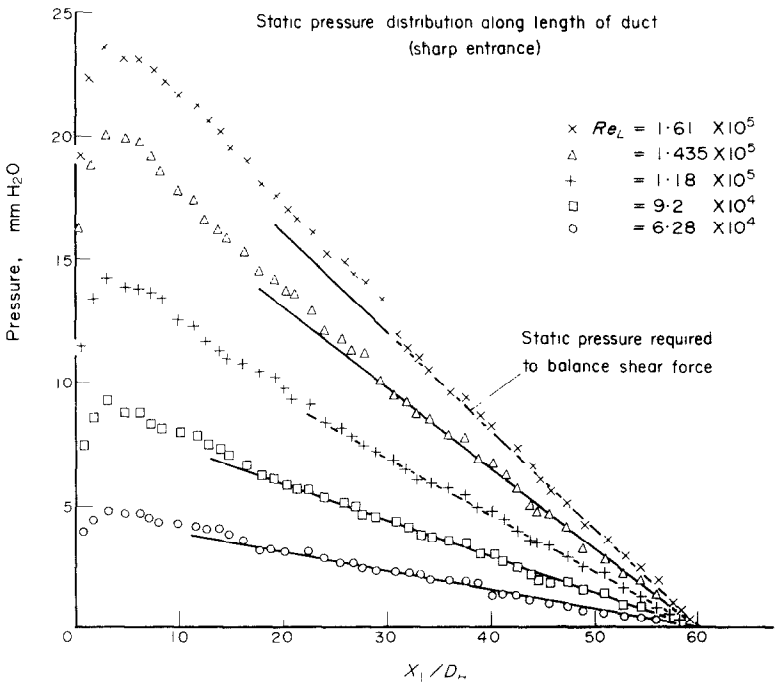

FIG. 3(b). Experimental static pressure distribution in the developing region for a sharp entrance.

region. Additional isovels at the four locations were obtained [14] for Reynolds numbers of $5{\cdot}9 \times 10^4$, $1{\cdot}41 \times 10^5$ and $1{\cdot}65 \times 10^5$, and indicate that the rate of development of the boundary layer increases with decreasing Reynolds number, as would be expected.

Static pressure distributions along the duct for a gradual entry were obtained for a range of Reynolds numbers and are shown in Fig. 3(a). The point of fully developed flow cannot be determined exactly for a particular Reynolds number, but the trend is for the development directly dependent on the Reynolds number, but in all the cases, it is smaller than for a gradual entry. This reduction is undoubtedly influenced by the vena contracta effect at the entry, which accelerates the core flow and produces a significant velocity defect thickness. This is a significant observation since many practical flow applications involve sharp entry conditions. The reduced development length means that the fully developed shear stress correlations can be applied with acceptable accuracy to the flow even earlier than for a

well-rounded entrance and are valid for $x_1/D_H > 5$. These experimental data and conclusions are consistent with the results of the following momentum analysis.

A momentum integral prediction method for the developing region of regular polygons

It is the purpose here to present an integral prediction approach for all regular polygons which incorporates the circle treated by Deissler [15]. The method gives the overall characteristics of the flow through regular polygons along the developing region. The method of obtaining the friction factor along the length, requires the initial and final velocity profiles to be known in terms of U_1^+ and x_2^+. Any intermediate velocity profile is assumed to be a combination of the two. The required assumptions are that the isovels are one dimensional, i.e. they are parallel to the boundary, and that the peripheral shear distribution is constant. These assumptions are quite well justified in the near wall region, by the experimental observations of the preceding section. Since the method has been restricted to regular polygons, only one half of a triangle with the base as a side of the polygon and the centroid as the vertex need be considered, see Fig. 4.

Assuming a uniform velocity profile at the entry, the boundary layer develops along the walls and the core flow is accelerated to accommodate the increasing displacement thickness. A force balance is taken in the longitudinal direction across an elemental length dx_1. The rate of change of momentum in slice dx_1 of the boundary layer is equal to the external forces acting on it in the x_1 direction, thus

$$-dP.(D-\delta/\tan\theta).\delta/2-\tau_w.dx_1.D/2$$

$$=d\left[\int_{(D\tan\theta/2)-\delta}^{D\tan\theta/2}\rho U_1^2\frac{x_2}{\tan\theta}dx_2\right]$$

$$-U_G\,d\left[\int_{(D\tan\theta/2)-\delta}^{D\tan\theta/2}\rho U_1\frac{x_2}{\tan\theta}dx_2\right] \quad (1)$$

where x_3 has been replaced by $x_2/\tan\theta$.

In the core region, assuming potential flow,

$$dP=-\rho U_G\,dU_G.$$

Thus

$$\frac{\rho U_G}{2}\left(D-\frac{\delta}{\tan\theta}\right)\delta\,dU_G-\tau_w\,dx_1\frac{D}{2}$$

$$=d\left[\int_{(D\tan\theta/2)-\delta}^{D\tan\theta/2}\rho U_1^2\frac{x_2}{\tan\theta}dx_2\right]$$

$$-U_G\,d\left[\int_{(D\tan\theta/2)-\delta}^{D\tan\theta/2}\rho U_1\frac{x_2}{\tan\theta}dx_2\right]. \quad (2)$$

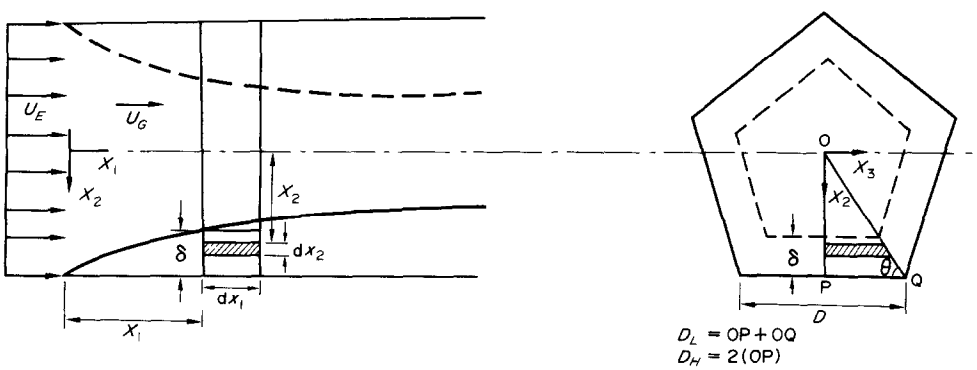

FIG. 4. Descriptive sketch of nomenclature used for integral momentum analysis.

Re-arranging and expressing the equation in non-dimensionalized form and integrating yields,

$$\frac{x_1}{D} = \int_{U_E^+ D^+}^{U_G^+ D^+} \left[\frac{U_G^+}{D^{+3}} \left(D^+ - \frac{\delta^+}{\tan\theta} \right) \delta^+ - \frac{2}{D^{+3}} \left(\int_{(D^+ \tan\theta/2) - \delta^+}^{D^+ \tan\theta/2} \times U_1^+ \frac{x_2^+}{\tan\theta} \mathrm{d}x_2^+ \right) \right] \mathrm{d}(U_G^+ D^+) + \int_0^b \frac{2}{D^{+2}} \mathrm{d} \left[\int_{(D^+ \tan\theta/2) - \delta^+}^{D^+ \tan\theta/2} \times (U_G^+ - U_1^+) \frac{U_1^+ x_2^+}{\tan\theta} \mathrm{d}x_2^+ \right] \quad (3)$$

where 'b' is the upper limit of the independent variable.

In the above expression, for the integration it is necessary that D^+ be known in terms of δ^+, and that U_1^+ be known in terms of x_2^+. The first requirement is obtained by the condition of conservation of mass, where the average velocity U_M remains the same along the tube formed by the triangle under consideration in the duct.

$$\frac{\rho U_M}{2} \frac{D}{2} \cdot \frac{D}{2} \tan\theta = \int_{(D \tan\theta/2) - \delta}^{D \tan\theta/2} \times \rho U_1 \frac{x_2}{\tan\theta} \mathrm{d}x_2 + \frac{\rho U_G}{2} \left(\frac{D \tan\theta}{2} - \delta \right)^2. \quad (4)$$

$$U_M^+ D^+ \tan\theta = \frac{8}{D^+ \tan\theta} \int_{(D^+ \tan\theta/2) - \delta^+}^{D^+ \tan\theta/2} \times U_1^+ x_2^+ \mathrm{d}x_2^+ + \frac{4U_G^+}{D^+ \tan\theta} \left(\frac{D^+}{2} \tan\theta - \delta^+ \right)^2. \quad (5)$$

The above equation relates δ^+ to D^+. The second requirement of equation (3) is for a knowledge of the dependence of U_1^+ on x_2^+. For this requirement a logarithmic profile is assumed.

Now since the hydraulic diameter $D_H = D \tan\theta$. The Reynolds number based on the hydraulic diameter becomes

$$Re_H = \frac{U_M D_H}{\nu} = U_M^+ D_H^+ = U_M^+ D^+ \tan\theta.$$

Substituting this in the mass conservation equation yields

$$Re_H = \frac{8}{D^+ \tan\theta} \int_{(D^+ \tan\theta/2) - \delta^+}^{D^+ \tan\theta/2} U_1^+ x_2^+ \mathrm{d}x_2^+ + \frac{4U_G^+}{D^+ \tan\theta} \left(\frac{D^+ \tan\theta}{2} - \delta^+ \right)^2. \quad (6)$$

Now the friction factor can be defined as

$$\frac{C_f}{2} = \frac{\tau_w}{\rho U_M^2} = \frac{1}{U_M^{+2}} = \frac{D^{+2} \tan^2\theta}{Re_H^2}. \quad (7)$$

Equation (3) can be re-written as

$$\frac{x_1}{D_H} = \frac{1}{\tan\theta} \left\{ \int_{U_E^+ D^+}^{U_G^+ D^+} \left[\frac{U_G^+}{D^{+3}} \left(D^+ - \frac{\delta^+}{\tan\theta} \right) \delta^+ - \frac{2}{D^{+3}} \left(\int_{(D^+ \tan\theta/2) - \delta^+}^{D^+ \tan\theta/2} U_1^+ \frac{x_2^+}{\tan\theta} \mathrm{d}x_2^+ \right) \right] \mathrm{d}(U_G^+ D^+) \int_0^b \frac{2}{D^{+2}} \mathrm{d} \left[\int_{(D^+ \tan\theta/2) - \delta^+}^{D^+ \tan\theta/2} (U_G^+ - U_1^+) \times \frac{U_1^+ x_2^+}{\tan\theta} \mathrm{d}x_2^+ \right] \right\}. \quad (8)$$

Hence, by numerically integrating equations (6)–(8), for a particular Reynolds number, the friction factor $C_f/2$ may be obtained for any regular polygon-shaped duct. For various values of δ^+, D^+ is obtained from equation (6). Now for specified values of Re_H, δ^+ and D^+: $C_f/2$ and x_1/D_H can be obtained from equations (7) and (8) respectively. Computational results and

data are plotted in Fig. 5, for the Reynolds number based upon a more realistic length scale D_L, defined with reference to Fig. 4 as

$$D_L = \text{OP} + \text{OQ}. \quad (9)$$

In all regular polygons D_L is greater than D_H, with the difference decreasing as the number of sides increases. The experimental correlations of shear stress were significantly improved for the square duct for Reynolds number based upon D_L rather than upon D_H. [14]

Finally, by neglecting the existence of secondary flows, a more general method [10] may be employed for the same predictions. For economy in computing time it is likely that the initial estimate of the longitudinal pressure gradient must be very good. The resulting velocity distribution predictions would have to be interpreted with the earlier neglect of the secondary flows in mind.

CONCLUSIONS

Developing flow in a square conduit has been examined experimentally and found to consist of a rapidly stabilsed 'near wall' layer, and an accelerating core. With increasing development length, or decreasing Reynolds number the boundary layer increases in thickness until the duct centerline is reached, then no further axial acceleration of fluid occurs. The pressure gradient in the developing region consists of two components, one related to the wall shear stress, and the other to the axial acceleration. By Preston tube measurements,

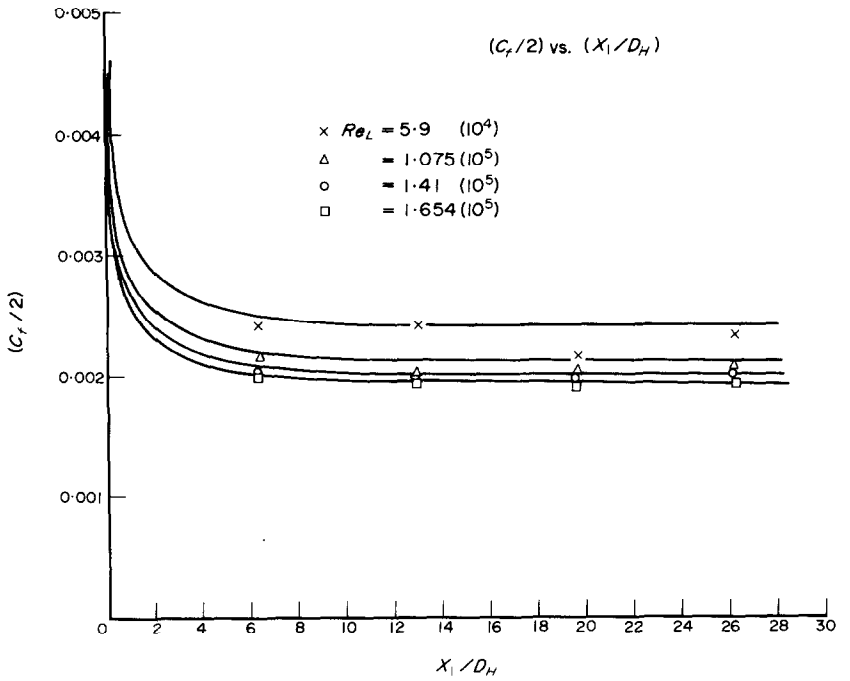

FIG. 5. The comparison of experimental and predicted values of C_f at various Reynolds numbers, Re_L.

it is observed that the wall shear stress rapidly approaches the fully developed value, and for engineering calculations this value can be adopted for distances greater than five hydraulic diameters from the inlet. An approximate momentum integral method is outlined which successfully correlates the wall shear coefficient in the development region for the range of experimental data. In addition, lateral wall shear stress data are presented for various Reynolds numbers and development lengths. The data indicated that the wall shear stress is very nearly uniform around the duct perimeter in the developing region, except for a small distance at the corners. Finally, both the experimental and the analytical friction coefficient data are compared with satisfactory accuracy when a new characteristic duct length is used that is defined for regular polygons.

ACKNOWLEDGEMENTS

The authors are indebted to the National Research Council of Canada for operating grant no. A2152 which financed this project.

REFERENCES

1. H. BLASIUS, Mitt. Forschung, *Ver. deut. Ing.* **131**, 1–34 (1913).
2. H. C. CLAIBORNE, A critical review of the literature on pressure drop in non circular ducts and annuli, Oakridge National Laboratory, ORNL Rep. 1248 (1952).
3. L. W. CARLSON and T. F. IRVINE JR., Fully developed pressure drop in triangular-shaped ducts. *J. Heat Transfer* **83**, 441 (1961).
4. E. R. G. ECKERT and T. F. IRVINE JR., Flow in corner of passages with non circular sections. *Trans Am. Soc. Mech. Engrs* **78**, 709–718 (May 1956).
5. J. NIKURADSE, Untersuchungen uber die Geschwindigteitsverteilung in turbulenten Stromungen, Thesis, Gottingen, (1926). V.D.I. Forsch 281.
6. L. PRANDTL, Uber die ausgebildete turbulenz, Proceedings, 2nd International Conference for Applied Mechanics, Zurich, Switzerland (1927).
7. L. C. HOAGLAND, Fully developed turbulent flow in rectangular ducts—secondary flows, its cause and effect on the primary flow, Ph.D. thesis, Dept. of Mech. Eng., Massachussetts Institute of Technology (1960).
8. E. BRUNDRETT and W. D. BAINES, The production and diffusion of vorticity in duct flow. *J. Fluid Mech.* **19** (Part 3), 375–392 (1964).
9. R. G. DEISSLER and M. F. TAYLOR, Analysis of turbulent flow and heat transfer in non circular passages, NASA TR R-31 (1958).
10. S. V. PATANKAR and D. B. SPALDING, A finite-difference procedure for solving the equations of the two dimensional boundary layer. *Int. J. Heat Mass Transfer* **10**, 1389–1412 (1967).
11. A. D. GOSSMAN, W. M. PUN, A. K. RUNCHAL, D. B. SPALDING and M. WOLFSHTEIN, *Heat and Mass Transfer in Recirculating Flows*. Academic Press, London (1969).
12. F. A. MACMILLAN, Experiments on Pitot-tubes in shear flow, Aero. Research Council, Gt. Britain, R & M 3028 (1957).
13. V. C. PATEL, Calibration of the Preston tube and limitation on its use in pressure gradients. *J. Fluid Mechanics* **23** (Part 1), 185–208 (1965).
14. S. AHMED, Turbulent flow in non circular ducts, Ph.D. thesis, Dept. of Mech. Engng, Univ. of Waterloo, Waterloo, Ontario, Canada (1970).
15. R. G. DEISSLER, Analysis of heat transfer and flow in the entrance regions of smooth passages, NACA Technical Note 3016 (1953).

ECOULEMENT TURBULENT DANS DES CONDUITS NON CIRCULAIRES

Résumé—Les principales propriétés généralisées de l'écoulement turbulent dans des conduits non circulaires sont examinées pour la région en développement dans un conduit carré. Les résultats expérimentaux renferment des profils de vitesse moyenne et des distributions de tensions périphériques pariétales à plusieurs endroites, aussi bien que la distribution longitudinale de pression statique, pour des nombres de Reynolds entre 50000 et 150000.

Il existe une similitude par les courbes isovitesses et de distribution des tensions pariétales entre la région d'établissement et celle de l'écoulement pleinement établi. La contrainte tangentielle pariétale prend rapidement une valeur qui est légèrement plus grande que celle pour un écoulement totalement développé, bien que le gradient de pression axiale ne soit pas stabilisé à cause de l'accélération convective du coeur du fluide. Ceci indique que l'écoulement proche de la paroi atteint rapidement des propriétés totalement développées.

Il est recommandé pour des calculs d'engineering qu'une longueur d'établissement dans des conduits soits définie en termes de stabilisation des parametres pariétaux tels ques la contrainte tangentielle et le transfert thermique. Pour le conduit carré avec entrée convergente à large rapport de contraction, la

contrainte tangentielle pariétale est établie pour six diamètres hydrauliques tandis que par comparaison le coeur du fluide nécessite une longueur de développement d'un ordre de grandeur plus élevé, qui devrait être contrôlé par le nombre de Reynolds. Les résultats de contrainte tangentielle relatifs au tube de Preston sont confirmés par un procédé d'intégration de quantité de mouvement qui est généralisé pour tous les polygônes réguliers. Les résultats expérimentaux et calculés de contrainte tangentielle pariétale sont en accord à 4 pour cent près avec les résultats de l'écoulement totalement établi dans un tuyau en utilisant une nouvelle échelle de longueur caractéristique qui tient compte de la forme du conduit.

TURBULENTE STRÖMUNG IN NICHT-KREISFÖRMIGEN RÖHREN

Zusammenfassung—Die verallgemeinerten zeitlichen Mittelwerte einer turbulenten Strömung in nicht-kreisförmigen Röhren wurden untersucht für die Anlaufzone eines Rohres mit quadratischem Querschnitt. Die experimentellen Daten umfassen Geschwindigkeitsprofile, Wandschubspannungen an verschiedenen Stellen und die Verteilung des statischen Druckes über der Rohrlänge; die Reynoldszahlen liegen dabei zwischen 50000 und 150000.

Es existiert eine Ähnlichkeit für die Geschwindigkeitsverteilung an der Wand und für die Wandschubspannungsverteilung in der Anlaufzone mit den Verhältnissen in der voll ausgebildeten Strömung. Die Wandschubspannung erreicht sehr rasch einen Wert, der etwas höher ist als der für voll ausgebildete Strömung, obwohl sich der Gradient des statischen Druckes noch nicht stabilisiert hat, was durch die konvektive Beschleunigung der Kernströmung verursacht ist. Dies zeigt, dass die Strömung in der Nähe der Wand rasch das Verhalten der vollausgebildeten Strömung aufbaut.

Für ingenieurmässige Berechungen wird empfohlen, eine effektive Anlauflänge in Röhren durch die Stabilisierung der lokalen Wandparameter wie Schubspannung und Wärmeübergang festzulegen. Für das verwendete Rohr mit quadratischem Querschnitt und einer gut gerundeten Einlauföffnung mit hohem Kontraktionsverhältnis ist die Wandschubspannung innerhalb von sechs hydraulischen Durchmessern ausgebildet, während zum Vergleich die Kernströmung eine Anlauflänge von etwa einer Grössenordnung mehr benötigt und stärker von der Reynoldszahl abzuhängen scheint. Die experimentellen Daten für die Schubspannung im Preston-Rohr werden bestätigt durch eine Impuls-Integral-Prozedur, die für alle regulären Polygonfiguren verallgemeinert aufgestellt wurde. Die experimentellen und die berechneten Werte der Wandschubspannung stimmen innerhalb von 4 Prozent der Daten für die voll ausgebildete Rohrströmung überein, wenn man eine neue charakteristische Länge benutzt, die die Form des Rohrquerschnitts berücksichtigt.

ТУРБУЛЕНТНОЕ ТЕЧЕНИЕ В НЕКРУГЛЫХ ТРУБАХ

Аннотация—Рассмотрены обобщенные средние характеристики турбулентного течения в некруглых трубах для области стабилизации в канале квадратного сечения. Экспериментальные данные включают средние профили скорости и распределения напряжения трения по периметру стенки в различных участках, а также продольное распределение статического давления для чисел Рейнольдса от 50 000 до 150 000.

Существует аналогия между распределением осредненных изотах и касательных напряжений на стенке в области стабилизации и этими характеристиками для полностью развитого течения. Касательное напряжение на стенке быстро достигает значения несколько большего, чем для полностью развитого течения благодаря конвективному ускорению ядра жидкости, даже если аксиальное распределение давления не стабилизировалось. Это свидетельствует о том, что вблизи стенки течение быстро приобретает свойства полностью развитого потока.

Для инженерных расчетов рекомендуется определять эффективную длину участка стабилизации в каналах в виде стабилизации таких параметров стенки как касательное напряжение и коэффициент теплообмена. Для квадратного канала с большим относительным сужением входа и скругленными входными кромками касательное напряжение на стенке стабилизировалось на расстоянии шести гидравлических диаметров, тогда как для ядра потока эта длина стабилизации приблизительно на порядок больше и сильно зависит от числа Рейнольдса. Экспериментальные значения касательных напряжений в трубке Престона подтверждаются значениями, полученными методом интегральных моментов, обобщенного для всех правильных многогранников. Экспериментальные и расчетные значения касательных напряжений на стенке для полностью развитого потока в трубах, полученные с использованием нового характерного масштаба длины, учитывающего форму трубы, коррелируются с точностью до 4%.